

Oxidation Behavior of SiC Whisker Reinforced Mullite ($-ZrO_2$) Composites

H. Y. LIU,* K.-L. Weisskopf,† M. J. Hoffmann & G. Petzow

Max-Planck-Institut für Metallforschung, Institut für Werkstoffwissenschaften, Pulvermetallurgisches Laboratorium, Heisenbergstrasse 5, D-7000 Stuttgart 80, FRG

(Received 30 May 1989, revised version received and accepted 1 August 1989)

Abstract

The oxidation behavior of hot-pressed 20 vol% SiC whisker–mullite matrix (with and without 10 vol% ZrO_2) composites was investigated at 1000 and 1200°C in air for up to 100 h. The oxidation scales were examined by scanning electron microscopy and wavelength-dispersive X-ray analysis. The oxidation of both composites occurred slowly at 1000°C and rapidly at 1200°C. The outwards diffusion of impurity ions (Na^+ , K^+ , etc.) and Al ions in the mullite decreased the viscosity of the oxidation scale and increased the oxidation rates. The oxidation rates for the composite without ZrO_2 were slightly lower than for the composite with ZrO_2 , which was probably due to ZrO_2 which inhibits the crystallization of the oxide film.

Das Oxidationsverhalten von heißgepreßten SiC Whisker–Mullit Kompositkeramiken (mit und ohne 10 vol% ZrO_2 -Dispersion) wurde bei 1000 und 1200°C an Luft bis zu 100 h untersucht. Die entstandenen Oxidationsschichten wurden mit Hilfe der Rasterelektronenmikroskopie und der wellenlängen-dispersiven Röntgenanalyse charakterisiert. Die Oxidation beider Kompositzusammensetzungen war bei 1000°C gering, bei 1200°C oxidierten beide Komposite rasch. Die Diffusion von Verunreinigungen (Na^+ , K^+ , etc.) und von Al Ionen aus dem Mullit setzte die Viskosität der Oxidationsschicht herab, und erhöhte die Oxidationsraten. Die Oxidationsraten der Komposite ohne ZrO_2 waren etwas geringer als die mit ZrO_2 -Dispersion. Dies ist vermutlich auf die

* Permanent address Shanghai Institute of Ceramics, Academia Sinica, Changning Road 865 Shanghai 20050, People's Republic of China

† Present address, Daimler-Benz AG, Forschung und Technik, D-7000 Stuttgart 80, FRG

Verhinderung der Auskristallisation der Oxidationsschicht durch das ZrO_2 zurückzuführen.

Le comportement à l'oxydation de composites pressés à chaud contenant 20 vol% de whiskers de SiC dans une matrice de mullite (avec ou sans 10 vol% de ZrO_2) a été étudié à 1000°C et 1200°C dans l'air pour des durées allant jusqu'à 100 h. Les couches d'oxyde ont été examinées par microscopie électronique à balayage et par analyse de rayons X par dispersion de longueur d'onde. L'oxydation des deux composites se produit lentement à 1000°C et rapidement à 1200°C. La diffusion vers l'extérieur des impuretés (Na^+ , K^+ , etc.) et la teneur élevée en Al de la mullite diminue la viscosité de la couche d'oxyde et augmente la vitesse d'oxydation. Cette dernière est légèrement plus basse pour le composite sans ZrO_2 que pour celui qui en contient, ce qui est probablement dû au fait que ZrO_2 inhibe la cristallisation de la couche d'oxyde.

1 Introduction

The high-temperature use of SiC whisker-reinforced ceramic matrix composites in air is, to a large extent, determined by their oxidation resistance. Very little data on the oxidation of these composites exist in the literature.

Although the high-temperature oxidation behavior of SiC has been extensively studied, there is no general agreement regarding the rate-controlling process. The diffusion of oxygen through the oxidation scale was suggested to be the rate-controlling process in most of the investigations,^{1–3} in which low activation energy values in the region of 120 kJ/mol were obtained.

Singhal⁴ measured a high activation energy (481 kJ/mol) and concluded that the outward

diffusion of CO (g) from the SiC–SiO₂ interface appeared to be the rate-controlling process. The CO gas was thought to be produced by a passive oxidation reaction¹



Bubble formation is commonly observed in the oxidation scale on polycrystalline SiC, but is rarely formed on the scales of single crystal material. Mieskowski *et al*⁵ suggested that the bubbles resulted from preferential oxidation of C inclusions existing in SiC polycrystals. The formed CO (possibly SiO, too) is controlling the oxidation rate.

Schlichtung and Kriegsmann² pointed out, that, in the case of small amounts of additives (Al, B) and impurities, the diffusion of molecular oxygen through the oxidation scale is controlling the oxidation kinetics of hot-pressed SiC, increased amounts of additives or impurities may change the oxidation kinetics.

Costello and Tressler³ suggested that the diffusion of molecular oxygen through the oxidation scale controls the process up to 1200°C. At higher temperatures they assumed more complicated diffusion processes, depending on the crystallization behavior of the oxidation scale.

Singhal and Lange,⁶ showed that an increasing amount of Al₂O₃ additive lowers the viscosity of the scale and increases the oxidation rate. The impurities originally present, or intentionally added as sintering additives, segregated into the oxidation scale. The decreasing viscosity of the scale due to the redistribution of the impurities increases the transport of the oxygen through the scale.⁷

In all these investigations, oxidation kinetics approximately agreed with the parabolic law. Depending on the impurity or additive content and the type of material (pressureless sintered or hot-pressed), activation energies for the oxidation of SiC derived from the parabolic curves vary from 84 to 498 kJ/mol.

The oxidation of SiC whisker–mullite (–ZrO₂) composites will be a very complex microchemical process. Fine SiC whiskers were dispersed in a mullite and mullite–ZrO₂ matrix. In addition to

minor amounts of impurities, the mullite used in this work contains a large excess of Al₂O₃ (> 70 wt%) In some samples 10 vol% ZrO₂ was added as toughening agent.

Mullite, hot-pressed in a graphite die, has a black or grey color, which is believed to be due to the reaction with carbon.⁸ However, this color of hot-pressed mullite could become completely white after a heat treatment at 1370°C in air for 50 h, or extended exposure at 1450°C,⁸ there may be also some oxidation reaction in the mullite matrix itself during a heat treatment at lower temperatures (1000–1200°C) in air.

Thus, the objective of this investigation is to characterize the oxidation behavior of hot-pressed SiC whisker–mullite(–ZrO₂) composites. The influence of impurity ingredients, mullite matrix composition as well as ZrO₂ and whisker inclusions will be studied. Additionally, it is of primary interest to determine the maximum temperature for use of these composites in ambient air.

2 Experimental

2.1 Materials

The materials investigated are listed in Table 1, in which mullite (M) and mullite with 10 vol% ZrO₂ (M10Z) were selected to show the oxidation behavior of the matrix. The whisker containing composites are marked with M20SCW or M10Z20SCW.

The starting components for the materials were fused mullite (Dynamullit-351 mesh, Dynamit Noble AG D-5210 Troisdorf-Oberlar, FRG), ZrO₂ powder (SC 20, Magnesium Electron Ltd, Manchester, UK) and SiC whisker (Tokamax, Tokai Carbon Co Ltd, Tokyo, Japan). The composition of the fused mullite was, in wt%: 76.8 Al₂O₃, 22.9 SiO₂, 0.01 TiO₂, 0.05 Fe₂O₃, 0.20 Na₂O, 0.04 CaO and MgO.

The attrition milled powder or tumbled powder–whisker mixtures were cold-pressed in a steel die and then hot-pressed in a BN-washed graphite die under a pressure of 28.5 MPa in flowing Ar for 0.5 h.

Table 1. Description of the polycrystalline materials

| Material | Composition | Temperature | Density ρ (g/cm ³) | Color |
|-----------|--|-------------|--|---------------|
| M | Mullite | 1600°C | 3.15 | Black or grey |
| M10Z | Mullite + 10 vol% ZrO ₂ | 1550°C | 3.43 | Grey |
| M20SCW | Mullite + 20 vol% SiC whisker | 1600°C | 3.16 | Green |
| M10Z20SCW | Mullite + 10 vol% ZrO ₂ + 20 vol% SiC whisker | 1600°C | 3.43 | Green |

The hot-pressed samples were cut using a diamond saw to approximately 60 mm × 3.5 mm × 2.5 mm. The two major faces were ground parallel and polished. The specimens were cleaned with acetone, deionized water and isopropanol in an ultrasonic bath and then dried.

2.2 Oxidation

The oxidation experiments were performed in a horizontal alumina tube furnace using SiC heating elements, in which the specimens were placed in a clean alumina tube, with inside diameter of 4.5 mm, in an alumina boat. The hot zone was maintained at a temperature of 1000 ± 10°C and 1200 ± 10°C. The oxidized specimens were weighed on an analytical balance after cooling to room temperature. The oxidation scale were characterized using X-ray diffraction (XRD), energy dispersive X-ray analysis (EDX), wavelength-dispersive X-ray analysis (WDX) and scanning electron microscopy (SEM).

3 Results and Discussion

3.1 Oxidation kinetics

The weight gain versus time curves for M20SCW, M10Z20SCW, M and M10Z obtained from oxidation at 1000 and 1200°C in the tube furnace are shown in Figs 1 and 2. The weight gain data of M20SCW (≤25 h) approximately agree with the parabolic law, and an apparent activation energy of 222 kJ/mol is roughly estimated. The weight gain data of M10Z20SCW agree well with the parabolic law (Fig 3), and a value of 207 kJ/mol is obtained for the activation energy. The thickness change with time of the oxide scale of M20SCW (Fig 4) also agrees well with the parabolic law.

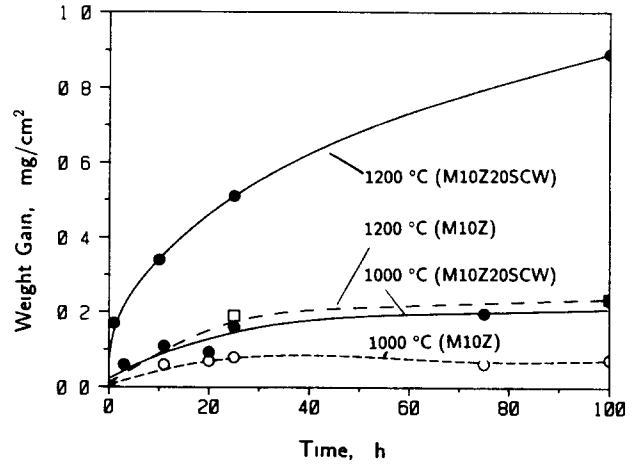


Fig. 2. Weight change versus time for the oxidation of the M10Z20SCW composite and of M10Z in air

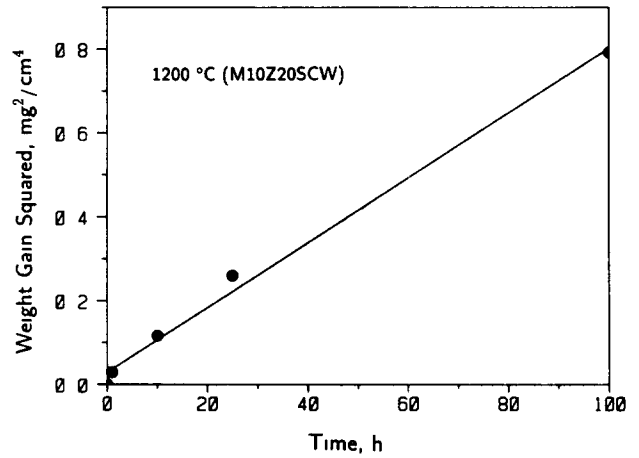


Fig. 3. Weight change versus time for the oxidation of the M10Z20SCW composite at 1200°C in air

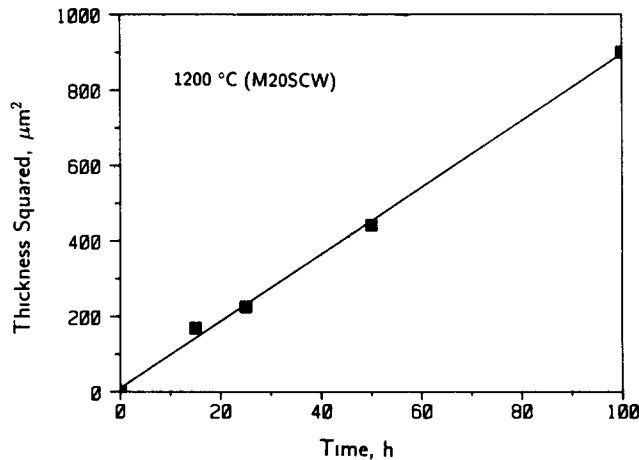


Fig. 4. Thickness change of the oxidized film as a function of time for the oxidation of the M20SCW composite at 1200°C in air

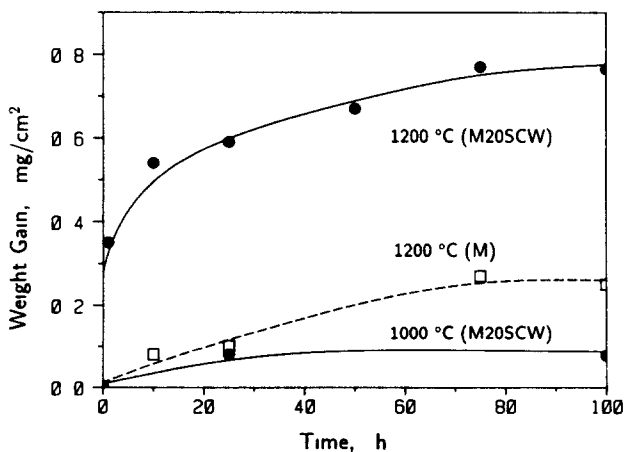


Fig. 1. Weight change versus time for the oxidation of the M20SCW composite and of mullite (M), in air

The surface and the fracture surface of the mullite matrix and the two composites exposed at 1000 and 1200°C in air are shown in Figs 5–10. For both composites, the oxidation rate at the higher temperature (1200°C) was initially high, since there is

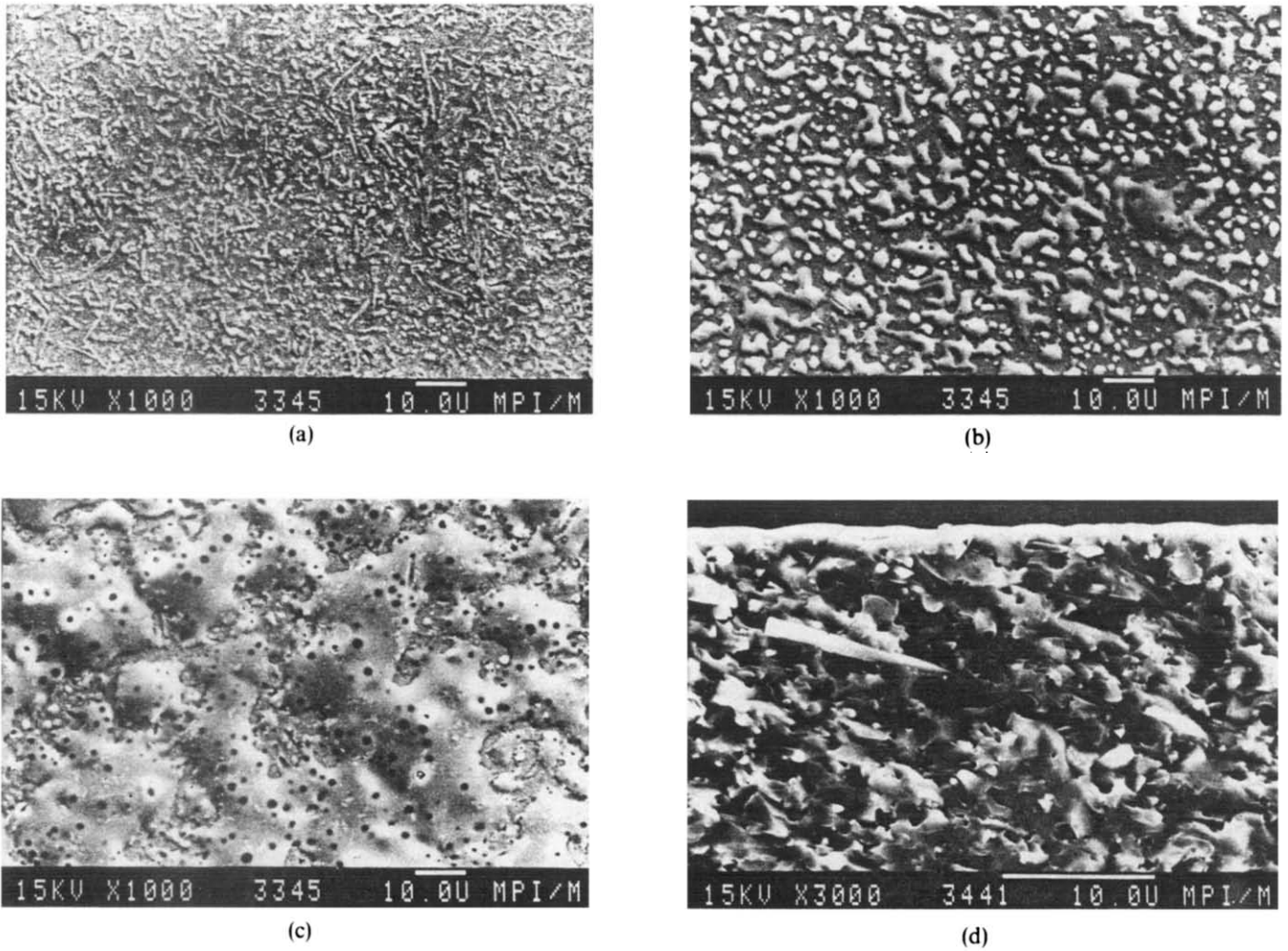


Fig. 5. Scanning electron micrograph of M20SCW samples oxidized during tests of high temperature bending strength (short exposure) at (a) 1000°C, (b) 1200°C, (c) 1300°C and (d) 1200°C, and then fractured at room temperature

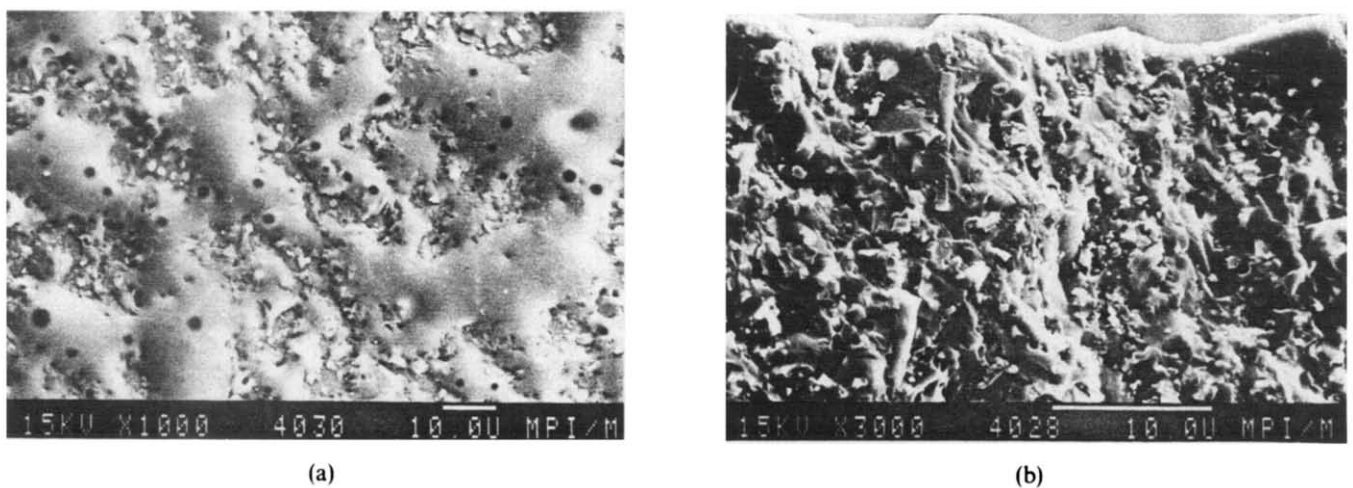
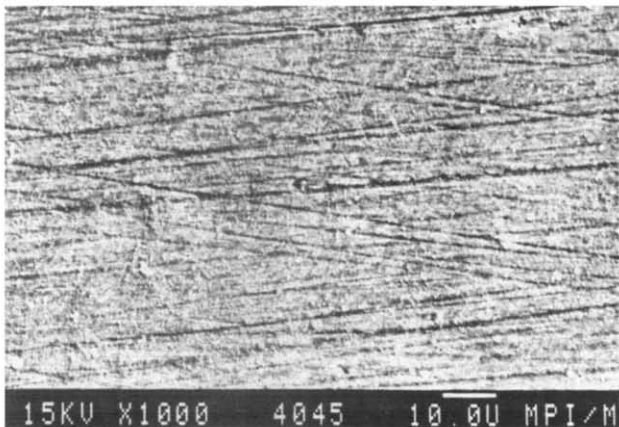
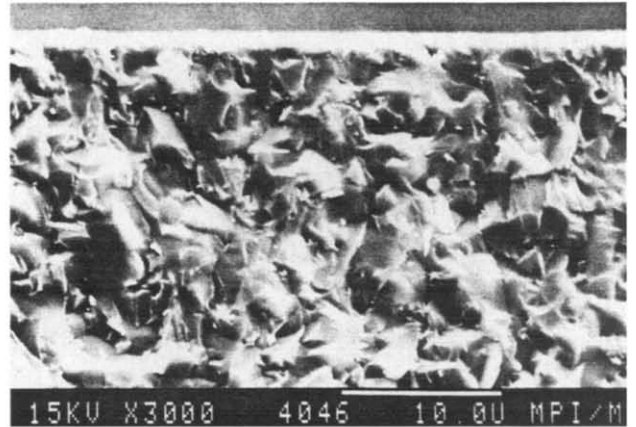


Fig. 6. Scanning electron micrographs of M20SCW oxidized at 1000°C in air for 100 h (a) surface, (b) fracture surface prepared after cooling

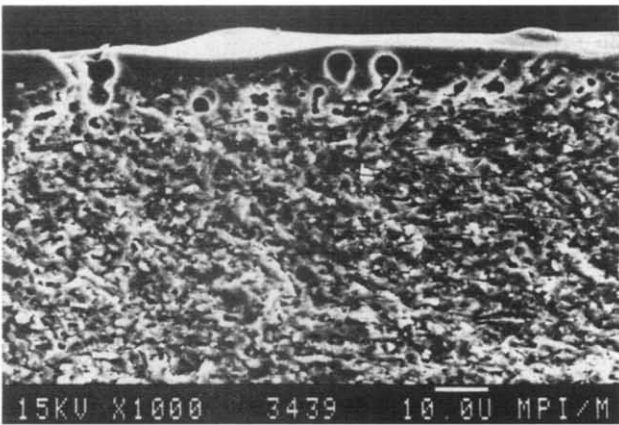


(a)

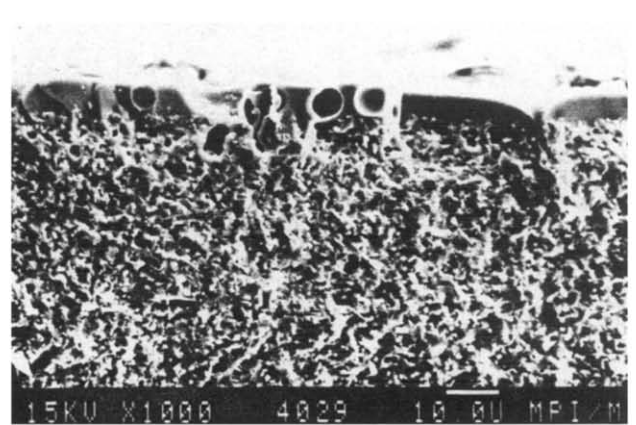


(b)

Fig. 7 Scanning electron micrographs of mullite oxidized at 1000°C in air for 100 h (a) surface, (b) fracture surface prepared after cooling

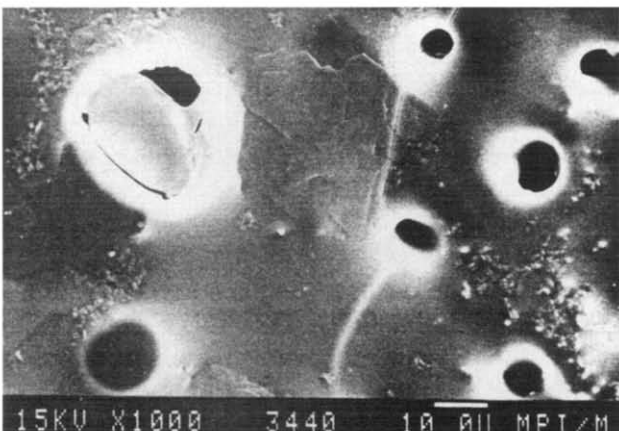


(a)

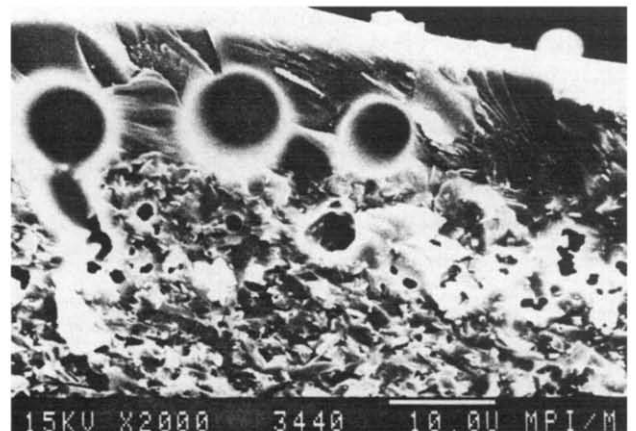


(b)

Fig. 8 Scanning electron micrographs of fracture surfaces of specimens oxidized at 1200°C in air for 15 h (a) M20SCW, (b) M10Z20SCW



(a)



(b)

Fig. 9 Scanning electron micrographs of M20SCW oxidized at 1200°C in air for 50 h (a) surface, (b) fracture surface prepared after cooling

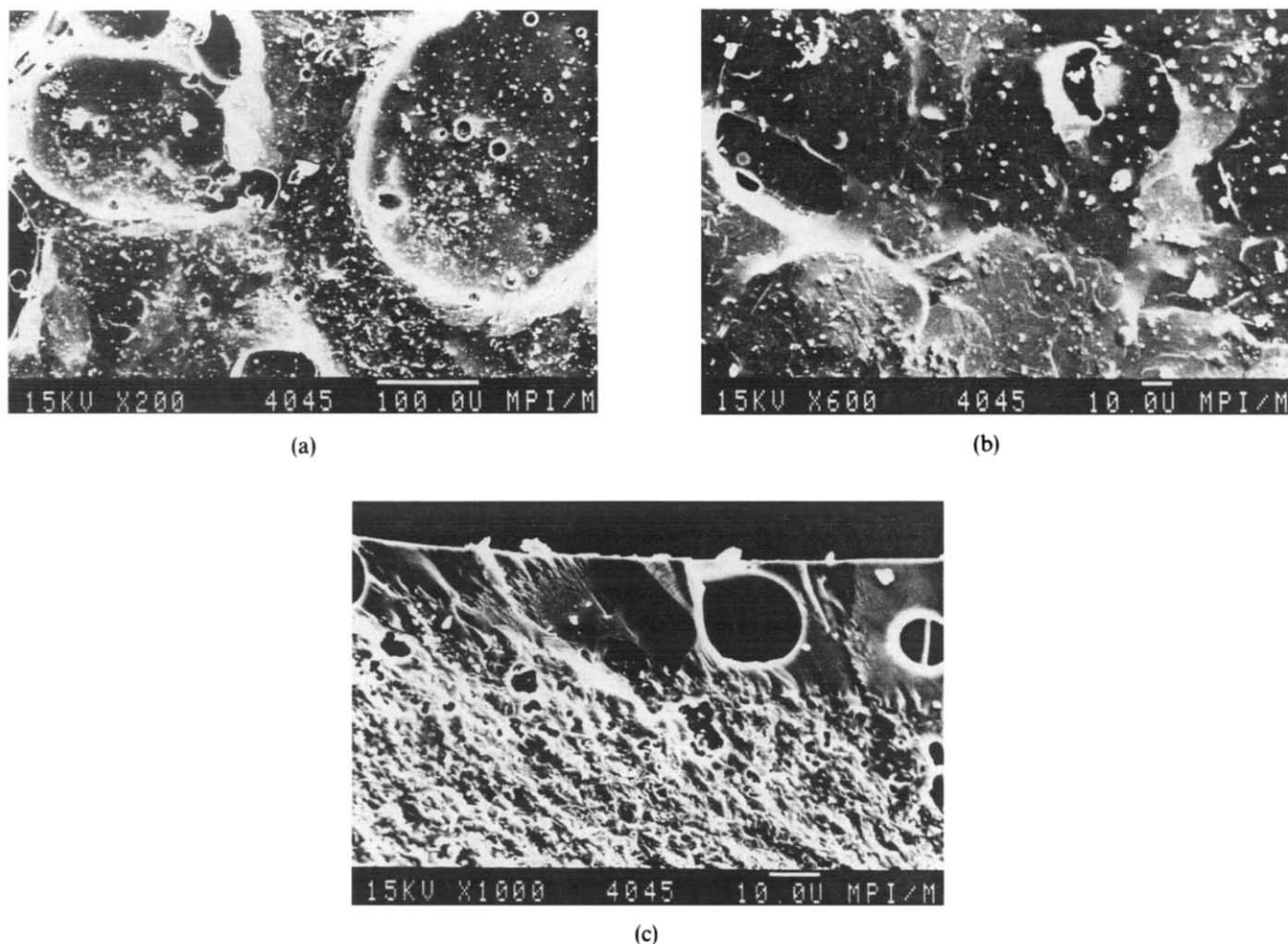


Fig 10. Scanning electron micrographs of M20SCW oxidized at 1200°C in air for 100 h (a) and (b) surface, (c) fracture surface prepared after cooling

no oxide film to protect the sectioned whiskers. This is shown in Figs 5(b) and (c). All the whiskers on the surface, which were directly exposed to air, reacted with oxygen forming a liquid phase, in several minutes. After the formation of a protective oxide film, a parabolic behavior was observed. At longer exposure time (≥ 25 h) crystallization of the oxide film on M20SCW occurred (Figs 9(a) and 10(b)), which may decrease the oxidation rate. On the other hand, bubbles and craters formed on the oxide film (Figs 8–10) suggest that rupturing of the oxidation scale by the escape of gaseous by-products may cause an increase in the oxidation rate. The samples exposed at 1200°C for a long time were difficult to handle. The thin glassy shells around the large bubbles on the oxidized surface were very easily broken, which leads to some scattering of the measured weight gain and scale-thickness change data.

As given in Table 2, the parabolic oxidation rate constants of the SiC whisker–mullite ($-\text{ZrO}_2$)

composites were one or two orders of magnitude higher than that of hot-pressed SiC ceramics found in the literature. This is consistent with the results reported by Borom *et al.*,⁹ that the oxidation rate of SiC in a mullite matrix is 10–20 times higher than that of pure SiC.

There were several reasons which were responsible for the high oxidation rates found. First, mullite showed an Al_2O_3 -rich stoichiometry, which may increase the parabolic rate constant as shown by Singhal and Lange on hot-pressed SiC.⁶ Borom *et al.*⁹ reported that the oxidized film on mullite with 20 vol% SiC whisker has a composition of 39 mol% Al_2O_3 and 61 mol% SiO_2 . Since this concentration lies below that required for stoichiometric mullite, a metastable eutectic around 1200°C¹⁰ or an immiscible alumino-silicate liquid¹¹ may occur. Secondly, Na, K and other impurities within the composite material segregated in the liquid film, lowering the silicate eutectic and the viscosity of the oxide film, and consequently increasing the oxidation rate.

Table 2. Comparison of oxidation rate constants

| Author | Material | Atmosphere | Oxidation temperature (°C) | Oxidation time (h) | Oxidation rate constant ($g^2/m^4 h$) |
|--|---|------------|----------------------------|--------------------|--|
| This work | M20SCW | Air | 1000 | 25 | 3.7×10^{-10} |
| | | | 1200 | 25 | 6.4×10^{-9} |
| | M10Z20SCW | Air | 1000 | 25 | 5.4×10^{-10} |
| | | | 1200 | 25 | 7.7×10^{-9} |
| Singhal and Lange (1975) ⁶ | HP-SiC + 1.8% Al ₂ O ₃ + 5.7% Al ₂ O ₃ + 11.0% Al ₂ O ₃ | Oxygen | 1370 | 22 | 6.9×10^{-9} 5.4×10^{-9} 2.4×10^{-8} |
| Singhal (1976) ⁴ | HP-SiC + 4% Al ₂ O ₃ | Oxygen | 1205 | 16 | 9×10^{-10} |
| | | | 1260 | | 2×10^{-9} |
| | | | 1315 | | 7×10^{-9} |
| | | | 1370 | | 2.2×10^{-8} |
| Schlichting and Kriegsmann (1979) ² | HP-SiC + 0.5% Al | Air | 1000 | 25 | 2.5×10^{-12} |
| | | | 1200 | | 6.4×10^{-11} |
| | | | 1400 | | 2.5×10^{-10} |
| | | | 1500 | | 1.9×10^{-10} |

M10Z20SCW had a slightly higher oxidation rate than M20SCW. This may be explained by the presence of ZrO₂. Compared to M20SCW a crystallization of the oxidation scale was not observed which gives reason to assume that the ZrO₂ retards the crystallization of the oxide film,¹² and probably decreases the viscosity of the liquid phase formed during the exposure.

3.2 Characterization of oxide films

XRD analysis of the oxide film formed on SiC whisker-mullite ($-ZrO_2$) composites at temperatures of 1000 and 1200°C revealed the presence of a glassy phase. No new crystalline phase, e.g., cristobalite or alumina, was identified in the oxide films. However, some precipitates in oxide films formed on M20SCW after the exposure of more than 25 h at 1200°C were observed by SEM and optical microscopy. These precipitates had to be mullite crystals, since only peaks of mullite were found. XRD analysis of the exposed matrix materials M and M10Z also revealed no new crystalline phases.

The morphologies of the oxide film formed on SiC whisker-mullite ($-ZrO_2$) composites are described in the following.

3.2.1 Beginning of oxidation

Before oxidation almost no contrast can be observed on a polished surface of M20SCW by SEM, since the atom masses of the elements contained in SiC whisker and mullite are similar. After exposure at 1000°C for several minutes (Fig. 5(a)), the shape of the SiC whisker can be observed. It indicated that at 1000°C the SiC whisker reacted mildly with oxygen.

At 1200°C (Fig. 5(b)), many small liquid drops, mostly less than 10 μm in size, were formed after several minutes. At 1300°C (Fig. 5(c)), there was more liquid phase formed with more gas pores, which connected each other and covered the surface. Figures 5(a)–(c) show that the temperature strongly affected the oxidation rate.

3.2.2 Oxidation at 1000°C

The liquid phase did not completely cover the surface of M20SCW oxidized at 1000°C for 100 h (Fig. 6(a)). There were small white particles distributed throughout the surface, which could not be identified by XRD or WDX. These particles may be aluminum silicate as reported by Singhal.⁴ Gas pores (bubbles), generated 2–3 μm below the surface, and the SiC whiskers located directly under the bubbles appeared unreacted (Fig. 6(b)). After the same exposure the surface and fracture surface of M10Z20SCW had a similar morphology as M20SCW. The mullite matrix specimens revealed no morphological change on the surface and the fracture surface (Figs. 7(a) and (b)).

3.2.3 Oxidation at 1200°C

The surface of M20SCW and M10Z20SCW oxidized for 15 h (Fig. 8) were uniformly covered with a smooth liquid film containing bubbles. The thickness of the films on both composites were about 13 μm. Many tiny pores were formed at the interface between the oxidation scale and the unoxidized part of the composites. Larger pores were formed in the oxidation layer during the escape of gaseous oxidation products.

Compared to the composites, mullite and M10Z specimens did not show any similar oxidation scales. The exposed mullite showed only a small amount of amorphous phase on the surface. On the M10Z samples no amorphous phase was observed, but grain growth and an effect similar to thermal etching of the grain boundaries was

After an exposure of 25 h the thickness of the oxide layer on M20SCW was $15\ \mu\text{m}$, and a small amount of precipitates in the amorphous layer was observed, the SiC whiskers in the volume of the sample retained their shape and appeared unoxidized

After an exposure of 50 h, crystallization and bubbles in the oxidation scale of M20SCW were observed (Fig 9(a)), the thickness of the layer was about $21\ \mu\text{m}$ (Fig. 9(b)).

The oxide layer on M20SCW oxidized for 100 h (Fig 10) was inhomogeneous. Locally, there were large bubbles or precipitates observed. The thickness of the scale varied on the surface (Fig 10(c)); a mean value of $30\ \mu\text{m}$ was estimated

In contrast, M10Z20SCW oxidized under the same conditions, showed a rather homogeneous oxidation layer with a larger number of small bubbles, however, no crystallization of the amorphous oxidation layer could be observed (Fig 11).

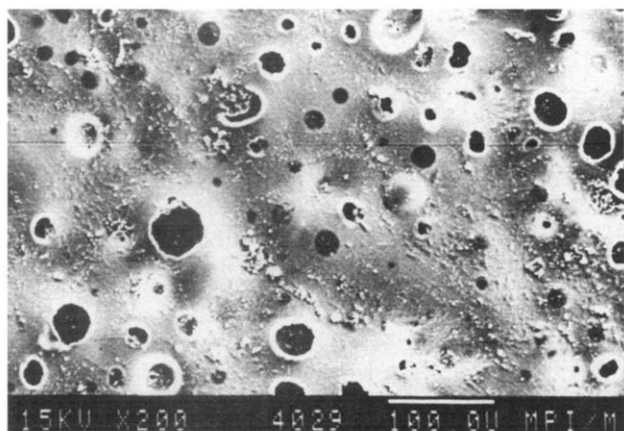
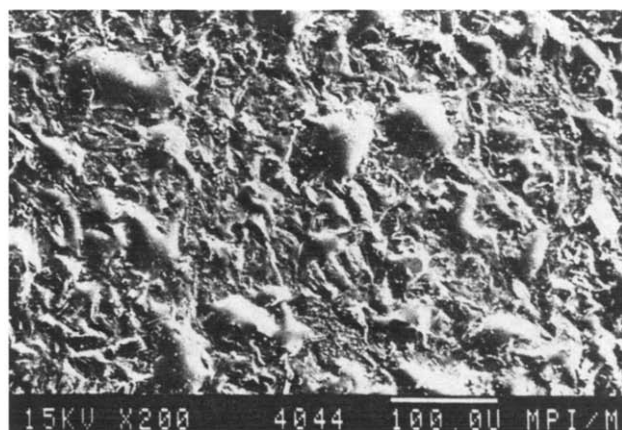
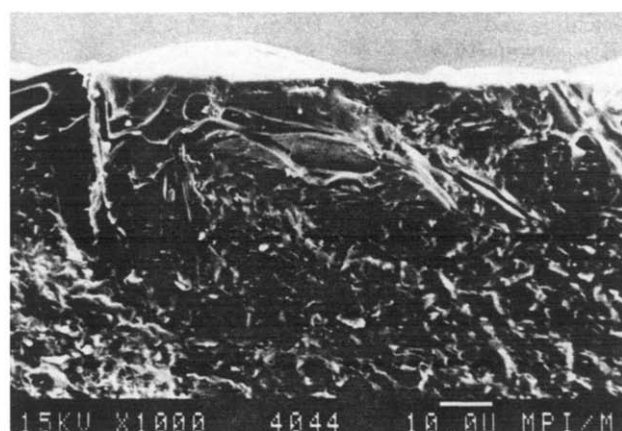


Fig. 11. Scanning electron micrograph of surface of M10Z20SCW oxidized at 1200°C in air for 100 h

On the surface of mullite samples oxidized for 100 h, an amorphous phase and abnormal grain growth was observed (Fig. 12). Large platelet grains were grown only near the surface and mostly below drops in the amorphous phase. The size of the inner grains remained unchanged (Fig. 12(b)). This indicates that the exaggerated grain growth, which is harmful to mechanical properties, is directly connected with the existing liquid phase. The M10Z



(a)



(b)

Fig. 12. Scanning electron micrograph of mullite (M) oxidized at 1200°C in air for 100 h

samples oxidized under the same conditions, show less grain growth on the surface. The ZrO_2 particles retard the formation of the glassy phase and inhibit the grain growth¹³

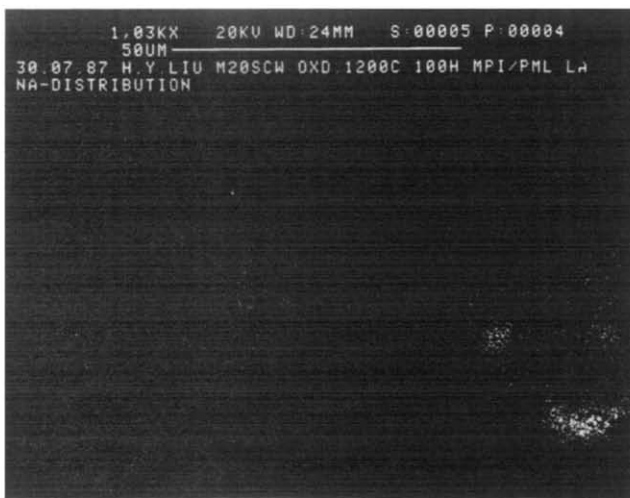
After the oxidation of 100 h at 1000 and 1200°C , mullite showed little or no change in color on the surface. However, the color of the surface of M10Z was changed from grey to white. A white oxidation layer along the surface could easily be seen by eye on the fracture surface of M10Z. This indicates that the presence of ZrO_2 increases the diffusion of oxygen through mullite, which is consistent with the weight gain curves.

EDX analyses performed on M20SCW oxidized at 1200°C for 25 h and at 1000°C for 100 h, showed only Si and Al peaks in the inside of the samples. Na, K and Ca peaks were detected in the oxidation layer.

Figures 13(a)–(c), show a polished cross section of M20SCW oxidized at 1200°C for 100 h, with Na and K maps obtained by WDX analyses. The Na- and



(a)



(b)



(c)

Fig. 13. (a) Polished cross section of M20SCW oxidized at 1200°C for 100 h, (b) Na map (wavelength dispersive), and (c) K map (wavelength dispersive) of sample shown in (a)

K-rich areas corresponded to the oxidation layer of 30 μm in thickness. Similar results were also obtained on the whisker-containing samples at other exposure conditions. Figures 14(a)–(c), show a polished cross section of M10Z20SCW oxidized at 1200°C for 100 h and the associated Na and Zr maps. The WDX analyses show an enrichment of the Na and Zr elements in the oxidation layer.

The diffusion processes which are responsible for the oxidation behavior of the SiC whisker–mullite ($-ZrO_2$) composites are shown schematically in Fig 15. The WDX analyses showed that the Na, K and other impurities, are concentrated in the oxidation layer of the samples by diffusion processes. The Na, K and other impurities originally existed in the mullite raw material, and attrition milling of the powder using a porcelain container resulted in further contamination. The diffusion of the oxygen to the inside, or the gaseous reaction products to the

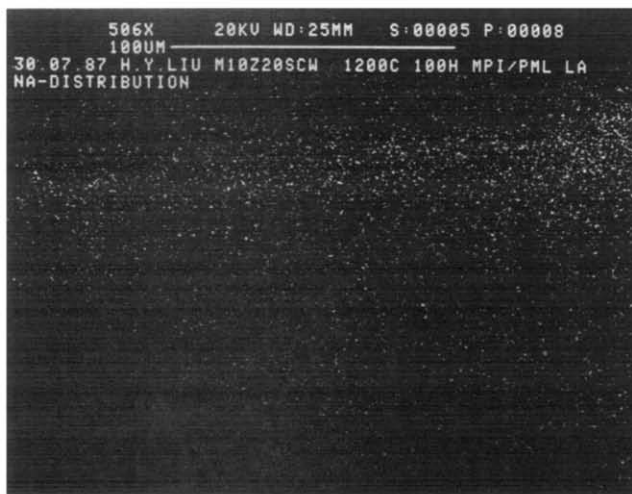
outside, is the rate-controlling process, which will be accelerated by the decrease of the viscosity of the oxide film. Because the elements Na and K are strongly decreasing the viscosity of a glassy phase and are concentrated in the oxidation layer, even the low concentration of these elements may be responsible for an increase of the oxidation rate.

The SEM investigations (Figs 8, 9(b) and 10(c)) showed that the growth of the oxidation scale is inhomogeneous. Tiny pores were observed between the matrix grains at the oxidation layer, indicating that oxygen diffuses along the grain boundaries and reacts with the SiC whiskers. The generally low activation energy of diffusion at interfaces compared to volume diffusion makes it plausible that the grain boundaries are rapid diffusion channels for the oxygen and the gaseous reaction products.

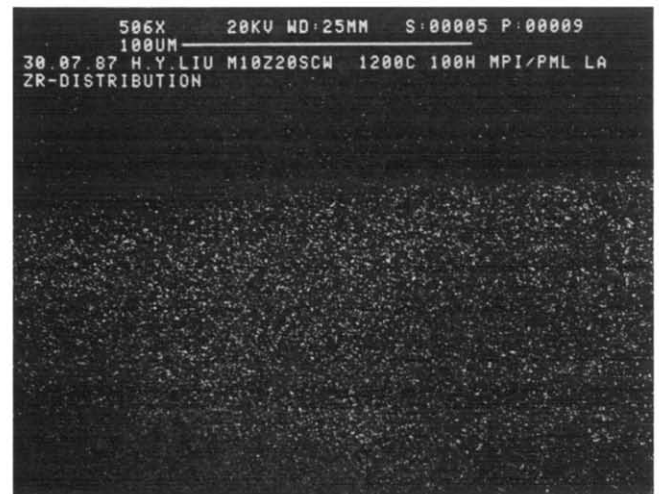
In both whisker composites the gaseous oxidation products caused sufficient internal pressure for the



(a)



(b)



(c)

Fig. 14. (a) Polished cross section of M10Z20SCW oxidized at 1200°C for 100 h, (b) Na map (wavelength dispersive), and (c) Zr map (wavelength dispersive) of sample shown in (a)

formation of small bubbles, which grow together to form larger ones during extended exposure, creating craters on the oxidized surface resulting in the escape of the gaseous reaction products. In this case the reduction of the viscosity of the glassy layer induced by the mobile impurity ions and the Al excess dissolved in the glassy phase plays an important role, too.

Our mechanical tests¹⁴ showed that the strength of the SiC whisker–mullite ($-\text{ZrO}_2$) composites decreased slightly from room temperature to 1000°C. The stronger degradation of strength at a test temperature $\geq 1200^\circ\text{C}$ in air is attributed to the residual glassy phase in the matrix and the oxidation of the SiC whiskers which accelerated slow crack growth.

4 Conclusions

Parabolic oxidation kinetics with moderate activation energies (220 and 207 kJ/mol) were observed for oxidation of M20SCW and M10Z20SCW. The oxidation behavior of these SiC whisker–mullite ($-\text{ZrO}_2$) composites is a diffusion-controlled process. However, it has not yet been determined whether the inwards diffusion of oxygen or the outwards diffusion of CO gas was the rate-controlling process. High contents of Al in the mullite favored the oxidation of the SiC whiskers. Segregation of Na and K impurities in the oxidation layer lowered the viscosity, increased the transport of oxygen and CO through the oxidation film, and thus increased the oxidation rate.

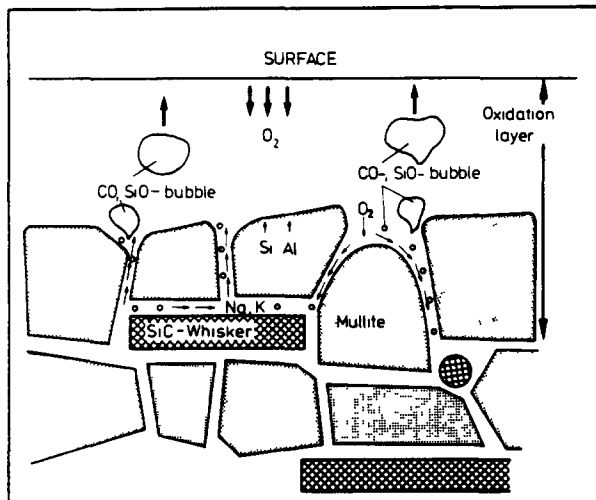


Fig 15. Schematic of the diffusion processes taking place during the oxidation of the SiC whisker-reinforced mullite composites

At 1000°C the composites were mildly oxidized. After 100 h their surfaces were only partly covered by a liquid film with tiny bubbles, and the thickness of the oxide layer was about $2\text{--}3\ \mu\text{m}$. At 1200°C the composites were severely oxidized and their surfaces were completely covered with a liquid film with large bubbles and craters. After extended exposure (25 h), crystallization in the oxidation layer was observed to some extent for M20SCW, but not for M10Z20SCW. ZrO_2 appeared to retard crystallization and slightly decreased the viscosity of the liquid film. Thus, ZrO_2 -containing SiC whisker-mullite composites (M10Z20SCW) had a slightly higher oxidation rate than that for M20SCW.

Compared to carbon fiber-reinforced ceramic composites the SiC whisker-mullite ($-ZrO_2$) composites have a much better oxidation resistance. The application of the whisker composites at 1000°C for long times seems to be possible, but the structural application of the composites at temperatures higher than 1000°C is limited by oxidation of the SiC whiskers. Reducing the alkali impurity content in the grain boundary phase, and the Al excess in the mullite, may improve the oxidation resistance of these composites. Further research is needed to understand the oxidation mechanisms, and to find appropriate routes to solve the oxidation problem.

Acknowledgements

The authors are grateful for financial support from the Federal Ministry for Science and Technology (BMFT) under the contract No 03 M10263. They would like to thank Professor Claussen for helpful discussions and Professor Brook for comments on this paper. The help of Miss Kuhnemann in the SEM analyses and Mr Labitzke in the WDX analyses are also greatly appreciated.

References

- 1 Motzfeld, K., On the rate of oxidation of silicon and silicon carbide in oxygen, and correlation with permeability of silica glass. *Acta Chem Scand*, **18** (1964) 1596.
- 2 Schlichting, J. & Kriegsmann, K., Oxidation behaviour of hot-pressed SiC. *Ber Dtsch Keram Ges*, **56**(3-4) (1979) 72-5.
- 3 Costello, J. A. & Tressler, R. E., Oxidation kinetics of hot-pressed and sintered α -SiC. *J Am Ceram Soc*, **64**(6) (1981) 327-31.
- 4 Singhal, S. C., Oxidation kinetics of hot-pressed silicon carbide. *J Mater Sci*, **11** (1976) 1246-53.
- 5 Mieskowski, D. M., Mitchell, T. E. & Heuer, A. H., Bubble formation in oxide scales on SiC. *J Am Ceram Soc*, **67**(1) (1984) C17-18.
- 6 Singhal, S. C. & Lange, F. F., Effect of alumina content on the oxidation of hot-pressed SiC. *J Am Ceram Soc*, **58**(9-10) (1975) 433-5.
- 7 Costello, J. A., Tressler, R. E. & Tsong, I. S. T., Boron redistribution in sintered α -SiC during thermal oxidation. *J Am Ceram Soc*, **64**(6) (1981) 332-5.
- 8 Prochazka, S. & Klug, F. J., Infrared transparent mullite ceramic. *J Am Ceram Soc*, **66**(12) (1983) 874-80.
- 9 Borom, M. P., Brun, M. K. & Szala, L. E., Kinetics of oxidation of carbide and silicide dispersed phases in oxide matrices. *Ceram Eng Sci Pro*, **8**(7-8) (1987) 654-70.
- 10 Aksay, A. & Pask, J. A., Stable and metastable phase equilibria in the system Al_2O_3 - SiO_2 . *J Am Ceram Soc*, **58**(11-12) (1975) 507-12.
- 11 MacDowell, J. F. & Beals, G. M., Immiscibility and crystallization in Al_2O_3 - SiO_2 glasses. *J Am Ceram Soc*, **52**(1) (1969) 17-25.
- 12 Sorrell, C. A. & Correll, C. C., Subsolidus equilibria and stabilization of tetragonal ZrO_2 in the system ZrO_2 - Al_2O_3 - SiO_2 . *J Am Ceram Soc*, **60**(11-12) (1977) 495-9.
- 13 Prochazka, S., Wallace, J. S. & Claussen, N., Microstructure of sintered mullite-zirconia composites. *J Am Ceram Soc*, **66**(8) (1983) C125-7.
- 14 Liu, H. Y., Weisskopf, K.-L. & Petzow, G., Hot-pressed SiC whisker-reinforced mullite ($-ZrO_2$) composites. *J Am Ceram Soc*, submitted.